Universal scaling of scattering observables for mass-imbalanced three-body systems

Lauro Tomio

ITA-DCTA and IFT-UNESP (Brazil)

Work done in collaboration with:
T. Frederico (ITA-DCTA, Brazil),
M. A. Shalchi and M.T. Yamashita (IFT-UNESP, Brazil),
M. R. Hadizadeh (Ohio University, USA),
E. Garrido (IEM-CSIC, SPain)

APFB2017, Guilin, China - August 26, 2017

Universal scaling of scattering observables for mass-imbalanced three-body systems

Main motivations are the present experimental possibilities:

(i) in nuclear physics, by considering halo-nuclei systems;
(ii) in cold-atom laboratories, when considering mixed atomic species.

In both the cases, our interest is to verify universal properties of scattering observables for three-body systems near the unitary limit.

Examples we are considering:

- **Halo-nuclei:** $n \to (n^{18}\mathrm{C})$
- **Ultracold atoms: The** $\alpha \to (\alpha\beta)$ **system, when** $m_\alpha \gg m_\beta$

Outline:

A) Weakly-bound nuclear systems: halo-nuclei

- The neutron$-{}^{19}$C elastic scattering near critical conditions for an excited ^{20}C state
  - Motivation based on related works in scattering with three-body systems and the Efimov states
  - Formalism for the scattering of a nucleon (n) by a dimer formed by $n-$core subsystem.
  - Scattering observables: $k\cot\delta_0$ and cross-section σ.
  - Results for $k\cot\delta_0$, considering zero-, low- and high-range two-body interactions.
  - Pole-positions of $k\cot\delta_0$, given as a function of E_{nc}.

B) Ultracold atoms: $\alpha \to (\alpha\beta)$ system, for $m_\alpha \gg m_\beta$

- Formalism follows the case $n \to (nc)$, except that the identical particles are not interacting.
- It is shown that the 3-body Efimov scaling factor can be well identified in $\alpha \to \alpha\beta$ scattering observables.
- As the scaling behavior is better verified for large imbalance-mass systems, the results can be relevant for the going-on experimental observations of Efimov physics in cold-atom laboratories.
- In case of $m_\alpha = 100\, m_\beta$, the ratio between consecutive levels of the bound-state energy spectrum is given by $\exp(2\pi/s_0) \sim 4.7$.
- Going to scattering region, the discrete Efimov scaling factor can also be well identified in scattering observables of one atomic species α when colliding with a two-body $\alpha\beta$ bound-state.

Motivations from ultracold atom laboratories

- Heidelberg group is studying the extreme mass-imbalance mixtures composed by ^{133}Cs and ^{6}Li atomic species [J. Ulmanis et al, PRL **117** (2016) 153201].
- Ultracold degenerate mixtures of alkali-metal-rare-earth molecules, ^{174,173}Yb$-^{6}$Li have also been considered by H. Hara et al [PRL **106** (2011) 205304] and Hansen et al [PRA **84** (2011) 011606(R)].
- Therefore, we understand that more favorable conditions are accessible to probe the rich Efimov physics in cold-atom laboratories.
- Note that, for the above mentioned examples, we have mass-ratios as m_β/m_α =0.034 for LiYb and 0.045 for LiCs

Universality in weakly-bound 3-body systems: Efimov physics

Efimov Effect: First predicted in 1970 by Vitaly Efimov (then at the Ioffe Physico-Technical Institute, St. Petersburg, Russia), when solving the quantum mechanics three-boson equation.

If two bosons interact in such a way that a two-body bound state is exactly on the verge of being formed, then in a three-boson system one should observe an infinite number of bound states. This phenomenon was shown that does not occur for less than three dimensions.

If one would be able to change the interaction strength, by making it either weaker or stronger, the number of three-body bound states would become finite.

The phenomenon is part of some general universal behavior of quantum few-body systems.

Why the actual interest?
Atomic physicists learned how to manipulate the interaction strength between atoms. Following that, several experimental groups obtain strong indications of three-body states as predicted by Efimov.

Search for Efimov states

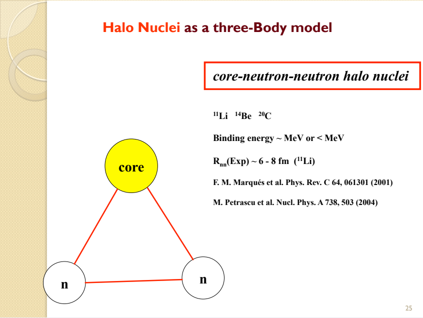

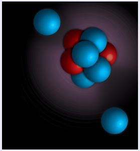

Properties of halo nuclei

- The radius of this kind of nuclei is much more than the expected value: $R = r_0 A^{1/3}$
- Weak interaction between the core and the halo-nucleons, such that we can consider a halo nuclei as three non-identical particle ($n - n -$core) system, and neglect the structure of the core.
- This three-body system has large two-body scattering lengths in comparison of the range of the interactions, suggesting the possibility of excited three-body Efimov states.

Efimov states in Halo Nuclei

Fedorov and Jensen, Phys. Rev. Lett. 25 (1993) 4103

Fedorov, Jensen, and Riisager, Phys. Rev. Lett. 73 (1994) 2817

Dasgupta, Mazumdar, and Bhasin, Phys. Rev. C 50 (1994) R550

VOLUME 73, NUMBER 21 PHYSICAL REVIEW LETTERS 21 NOVEMBER 1994

Efimov States in Halo Nuclei

D. V. Fedorov,* A. S. Jensen, and K. Riisager
Institute of Physics and Astronomy, Aarhus University, DK-8000 Aarhus C, Denmark
(Received 13 April 1994)

We investigate conditions for the occurrence of Efimov states in the recently discovered halo nuclei. These states could appear in systems where one neutron is added to a pronounced one-neutron halo nucleus. Detailed calculations of the properties of the states are presented and promising candidates are discussed.

PHYSICAL REVIEW C VOLUME 56, NUMBER 5 NOVEMBER 1997

Universal aspects of Efimov states and light halo nuclei (*)

A. E. A. Amorim,[1,2] T. Frederico,[3] and Lauro Tomio[1]

The parametric region in the plane defined by the ratios of the energies of the subsystems and the three-body ground state, in which Efimov states can exist, is determined. We use a renormalizable model that guarantees the general validity of our results in the context of short-range interactions. The experimental data for one- and two-neutron separation energies, implies that among the halo nuclei candidates, only ^{20}C has a possible Efimov state, with an estimated energy less than 14 KeV below the scattering threshold. [S0556-2813(97)50611-X]

Threshold conditions for an excited N+1 Efimov state

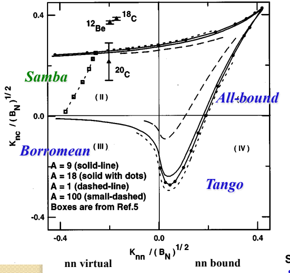

$K_2 = (E_2)^{1/2}$ (where 2 refers to n-n or n-c) and *B_N is the N-th 3body bound state.* *Here, it is shown the boundary of the region where the binding energy of the (N+1)th Efimov state is zero for different core masses (A).*
Negative values for the two-body observables correspond to virtual states.
It is also shown three experimental data, corresponding to the halo nuclei ^{20}C, ^{18}C, ^{12}Be [Audi and Wapstra, NPA595(1995)409].
The squares, connected with dashed lines, are obtained from Fig. 2 of Fedorov et al. PRL73(1994)2817.

See also Canham & Hammer "Universal properties and structure of halo nuclei", Eur. Phys. J. A **37**, 367 (2008)

(*) Work done as part of the PhD thesis of Amorim, from 1995 and 1996, submitted for publ. in 1996.

Threshold conditions and Scaling function

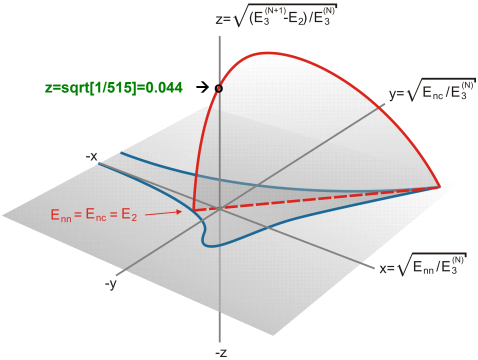

$$\boxed{\frac{B_3^{(N+1)}}{B_3^{(N)}} = F\left(\frac{K_{\alpha\alpha}}{\sqrt{B_3^{(N)}}};\frac{K_{\alpha\beta}}{\sqrt{B_3^{(N)}}};A\right),}$$

$$\boxed{A \equiv M_\beta / M_\alpha}$$

Exploring the Efimov physics: From bound to scattering

- Consider the general case of three-boson system with non-identical masses such that $m_\alpha \gg m_\beta$, when the two-body scattering length is close to infinite.
- Two levels of the 3-body spectrum are related by a scaling factor: $\exp(2\pi/s_0)$, where s_0 is a constant that varies according to the mass-ratio [See Braaten and Hammer, Phys. Rep. 428 (2006) 259].
- When all the sub-systems are interacting, the maximum energy-ratio at unitary limit occurs for $m_\alpha = m_\beta$, predicted to be ~ 515.
- When $m_\alpha = 100 m_\beta$, $\exp(2\pi/s_0) \sim 4.7$, with particular interest for experiments with cold atoms.
(We have also defined $m_H \equiv m_\alpha$ and $m_L \equiv m_\beta$, for atomic systems.)

Equal-mass case: Pole in $k\cot\delta$ for the $n-d$ system

- W.T.H. van Oers and J.D. Seagrave, Phys. Lett. B **24** (1967) 562.
  By analyzing data for $n - d$ scattering, they pointed out a pole in $k\cot\delta$.
- A.S. Reiner, Phys. Lett. B **28** (1969) 387.
  The anomalous effective range expansion of the doublet $n - d$ elastic scattering is due to a pole just below the threshold.
- J.S. Whiting and M.G. Fuda, Phys. Rev. C **14** (1976) 18.
  The pole position and residue was obtained from dispersion relation and exact solution of 3B equations.
- B.A. Girard and M.G. Fuda, Phys. Rev. C **19** (1979) 579.
  The existence of the triton virtual state was found on the basis of the effective range expansion.
- S.K. Adhikari, A.C. Fonseca, and LT, Phys. Rev. C **26** (1982) 77; S.K. Adhikari and LT, Phys. Rev. C **26** (1982) 83; S.K. Adhikari, LT and A.C. Fonseca, Phys. Rev. C **27** (1983) 1826.
  Studies on Efimov effect in the three-nucleon system. It was shown that the triton virtual state appears from an excited Efimov state moving to the non-physical energy sheet through the elastic cut.

PHYSICAL REVIEW C VOLUME 14, NUMBER 1 JULY 1976

Pole in $k \cot\delta$ for doublet, s-wave, n-d scattering

James S. Whiting and Michael G. Fuda
Department of Physics and Astronomy, State University of New York, Buffalo, New York 14214

(Received 23 March 1976)

The position of the pole in $k \cot\delta$, for doublet, s-wave, n-d scattering, and its residue are shown to be correlated with the doublet scattering length. An approximate, analytic solution of the N/D equations of Barton and Phillips indicates a linear dependence on the doublet scattering length for the pole position, and a
solutions of
nd to be
a for $k \cot\delta$,
formalism is
nd cut in an

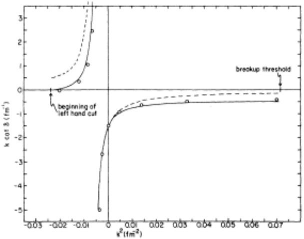

FIG. 3. $k \cot\delta$ for the doublet, s state as a function of k^2, where k is the relative wave number. Solid lines are from the exact N/D calculations. Dashed lines are from Eq. (25). Circles are for either separable potential. In all cases the doublet scattering length is 0.652 fm.

Unbalanced-mass case: Pole in $k\cot\delta$ for the halo-nuclei system

- M.T. Yamashita, T. Frederico and LT, Phys. Rev. Lett. **99** (2007) 269201; Phys. Lett. B **660** (2008) 339.
  Shows the migration of the excited Efimov state of $n-n-^{18}C$ to the virtual state, as well as performed calculations on the $n-^{19}C$ scattering within zero-range interaction.
- M.A. Shalchi, M.T. Yamashita, M.R. Hadizadeh, T. Frederico, LT, Phys. Lett. B **764** (2017) 196. Neutron$-^{19}$C scattering: Emergence of universal properties in a finite-range potential; Phys. Lett. B **771** (2017) 635 (Erratum).
- A. Deltuva, Phys. Lett. B **772** (2017) 657 Neutron$-^{19}$C scattering: Towards including realistic interactions.

Formalism

The amplitude of on–shell scattering of n from nc target;

$$h_n(q,E) = \mathcal{V}(q,k,E) + \frac{2}{\pi}\int dq'\, q'^2\, \frac{\mathcal{V}(q,q',E)h_n(q',E)}{q'^2 - k^2 - \mathrm{i}\epsilon}$$

- q: the momentum of the spectator particle (n) with respect to the CM of the $(n-c)$ subsystem.
- the on-energy-shell:
  $k \equiv |\vec{k}_i| = |\vec{k}_f| = \sqrt{[2(A+1)m/(A+2)]\,(E - E_{nc})}$

where

$$\begin{aligned}\mathcal{V}(q,q',E) &= \frac{\pi}{2}\bar{\tau}_{nc}(q) \\ &\times \left[K_2\,(q,q',E) + \int dk\, k^2\, K_1\,(q,k,E)\tau_{nn}(k)K_1\,(q',k,E)\right]\end{aligned}$$

For both $n-n$ and $n-c$ two-body interactions, we use one–term separable Yamaguchi-type potentials:

$$V(p,p') = \lambda \left(\frac{1}{p^2+\beta^2}\right)\left(\frac{1}{p'^2+\beta^2}\right),$$

where

$$\lambda = \frac{-2\pi\mu}{\beta(\beta \pm \kappa)},$$

and the range of the interaction

$$r_0 = \frac{1}{\beta} + \frac{2\beta}{(\beta \pm \kappa)^2},$$

$\bar{\tau}_{nc}$ and τ_{nn} (reflecting 2B t–matrices):

$$\begin{aligned}
\bar{\tau}_{nc}(q) &= \frac{-\beta_{nc}(\beta_{nc}+\kappa_{nc})^2(\beta_{nc}+\kappa_{3nc})^2(\kappa_{nc}+\kappa_{3nc})(A+1)^2}{\mu_{nc}\pi(2\beta_{nc}+\kappa_{3nc}+\kappa_{nc})A(A+2)} \\
\tau_{nn}(q) &= \frac{2\beta_{nn}}{\mu_{nn}\pi}\frac{(\beta_{nn}+\kappa_{nn})^2(\beta_{nn}+\kappa_{3nn})^2}{(-2\beta_{nn}-\kappa_{3nn}+\kappa_{nn})(\kappa_{nn}+\kappa_{3nn})},
\end{aligned}$$

where:

$$\begin{aligned}
\kappa_{nn} &= \sqrt{-mE_{nn}} \\
\kappa_{nc} &= \sqrt{-\frac{2mA}{A+1}E_{nc}} \\
\kappa_{3nn} &= \sqrt{-m(E-\frac{(A+2)q^2}{4Am})} \\
\kappa_{3nc} &= \sqrt{-\frac{2mA}{A+1}(E-\frac{(A+2)q^2}{2(A+1)m})}.
\end{aligned}$$

K_1 and K_2 functions:

$$K_1(q,q',E) = \int dx \frac{1}{E - \frac{q^2}{m} + \frac{q'^2(A+1)}{2Am} + \frac{qq'x}{m}} \times \left(q^2 + \frac{q'^2}{4} + qq'x + \beta_{nn}^2\right)^{-1} \left(q'^2 + \frac{q^2A^2}{(A+1)^2} + \frac{2qq'Ax}{(A+1)} + \beta_{nc}^2\right)^{-1}$$

$$K_2(q,q',E) = \int dx \frac{1}{E - \frac{q^2(A+1)}{2Am} - \frac{q'^2(A+1)}{2Am} + \frac{qq'x}{Am}} \times \left(q'^2 + \frac{q^2}{(A+1)^2} + \frac{2qq'x}{(A+1)} + \beta_{nc}^2\right)^{-1} \left(q^2 + \frac{q'^2}{(A+1)^2} + \frac{2qq'x}{(A+1)} + \beta_{nc}^2\right)^{-1}$$

Handling the singularities (in case of zero-range interactions) by a subtraction renormalization approach:

$$\begin{aligned}\Gamma_n(q,k;E) &= \mathcal{V}(q,k;E)\\ &+ \frac{2}{\pi}\int_0^\infty dp\left[p^2\mathcal{V}(q,p;E)-k^2\mathcal{V}(q,k;E)\right]\frac{\Gamma_n(p,k;E)}{p^2-k^2},\end{aligned}$$

$$h_n(q;E)=\frac{\Gamma_n(q,k;E)}{1-\frac{2}{\pi}k^2\int_0^\infty dp\,\frac{\Gamma_n(p,k;E)}{p^2-k^2-\mathrm{i}\epsilon}}.$$

On–shell scattering amplitude:

$$h_n(k;E) = [k\cot\delta_0 - \mathrm{i}k]^{-1},$$

where

$$k\cot\delta_0 = \frac{1}{\Gamma_n(k,k;E)}\left[1 - \frac{2}{\pi}k^2\int_0^\infty dp\,\frac{\Gamma_n(p,k;E)-\Gamma_n(k,k;E)}{p^2-k^2}\right].$$

Scattering differential cross section:

$$\frac{d\sigma}{d\Omega} = |h_n(k;E)|^2$$

Calculation of bound and virtual-states:

$$h_{nc}(q) = (q^2 - k_i^2)\chi_n(q) \quad , \quad h_{nn}(q) = \chi_c(q)$$

We have:

$$\begin{aligned} h_{nc}(q) &= \bar{\tau}_{nc}(q) \int dq'\, q'^2 \left(k_2\,(q, q', E) \frac{h_{nc}(q')}{q'^2 - k_i^2 + i\epsilon} + k_1\,(q, q', E) h_{nn}(q') \right) \\ h_{nn}(q) &= \tau_{nn}(q) \int dq'\, q'^2\, k_1\,(q', q, E) \frac{h_{nc}(q')}{q'^2 - k_i^2 + i\epsilon}, \end{aligned}$$

By going to the second sheet of the complex energy:

$$\begin{aligned} h_{nc}(q) &= \bar{\tau}_{nc}(q) [\pi k_v k_2\,(q, -ik_v, E) h_{nc}(-ik_v) \\ &+ \int dq'\, q'^2 \left(k_2\,(q, q', E) \frac{h_{nc}(q')}{q'^2 + k_v^2} + k_1\,(q, q', E) h_{nn}(q') \right)] \\ h_{nn}(q) &= \tau_{nn}(q) \left[\pi k_v k_1\,(-ik_v, q, E) h_{nc}(-ik_v) + \int dq'\, q'^2\, k_1\,(q', q, E) \frac{h_{nc}(q')}{q'^2 + k_v^2} \right], \end{aligned}$$

single equation for both bound and virtual states (l=b, v):

$$h_{nc}(q) = 2k_v \mathcal{V}\,(q, -ik_v, E) h_{nc}(-ik_v) \delta_{l,v} + \frac{2}{\pi} \int dq'\, q'^2\, \mathcal{V}\,(q, q', E) \frac{h_{nc}(q')}{q'^2 + k_l^2}$$

Typical values of Yamaguchi potential parameters to reproduce

- ground state binding energy of ^{20}C with $E = -3.5$ MeV
- nn virtual state energy with $E_{nn} = -143$ keV

	$\beta_{nn} = 1.34$ fm^{-1}		$\beta_{nn} = 24.5$ fm^{-1}	
$\lvert E_{^{19}C}\rvert$(keV)	β_{nc} (fm^{-1})	r_{nc} (fm)	β_{nc} (fm^{-1})	r_{nc} (fm)
200	0.971	2.736	18.970	0.157
400	0.754	3.233	17.036	0.174
600	0.598	3.720	15.592	0.190
800	0.477	4.255	14.395	0.205

Trajectory of 3B bound and virtual states

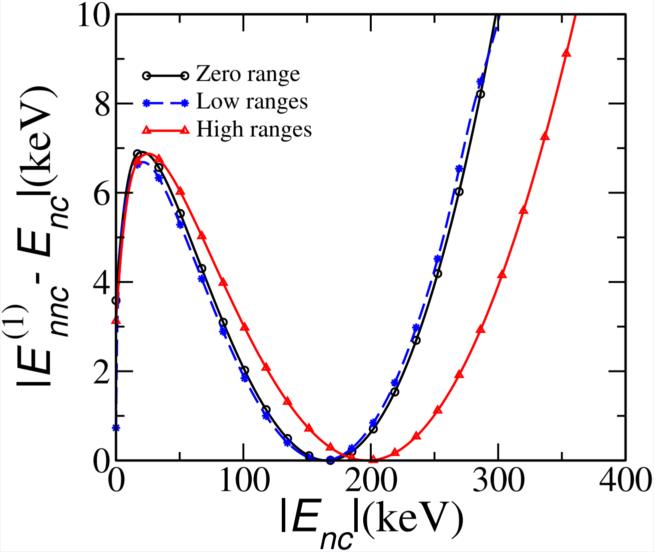

$k \cot \delta_0^R$ - Renormalized zero-range potential

- Results for $(1 - E_K/E_0) k \cot \delta_0^R$ as a function of the colliding neutron energy E_K, obtained with the renormalized zero–range potential. with corresponding fitting, where E_0 is the energy corresponding to the pole position, and $E_K \equiv k^2/(2\mu_{n,nc})$.
  The $n - c$ binding energies ($|E_{^{19}\mathrm{C}}|$), are given inside the panel.

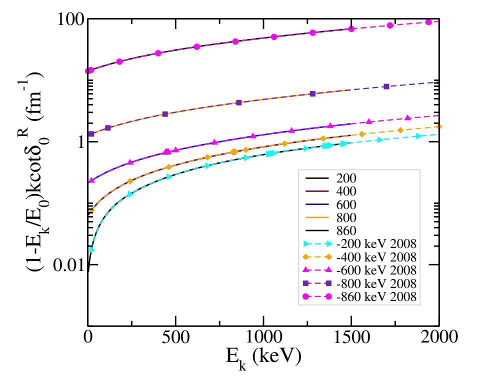

$k \cot \delta_0^R$, with finite low-range interactions (high values of β)

- Results for $(1 - E_K/E_0)k \cot \delta_0^R$ as a function of the colliding neutron energy E_K, considering a few values of $|E_{^{19}\mathrm{C}}|$, given inside the panel, obtained with the finite low-range potential (large βs), with corresponding fitting. E_0 is the energy corresponding to the pole position, and $E_K \equiv k^2/(2\mu_{n,nc})$.

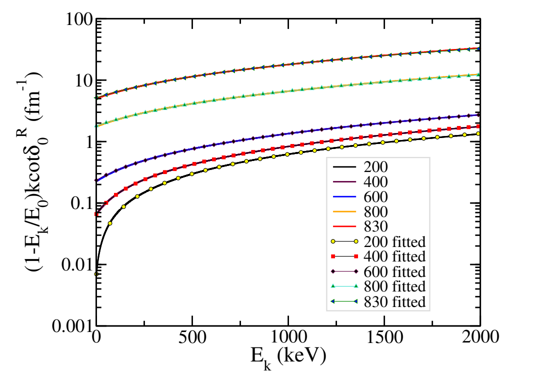

$k \cot \delta_0^R$, with finite high-range interactions (low values of β

- Results for $(1 - E_K/E_0) k \cot \delta_0^R$ as a function of the colliding neutron energy E_K, obtained with the finite high-range potential (low βs), with corresponding fitting. E_0 is the energy corresponding to the pole position, and $E_K \equiv k^2/(2\mu_{n,nc})$.

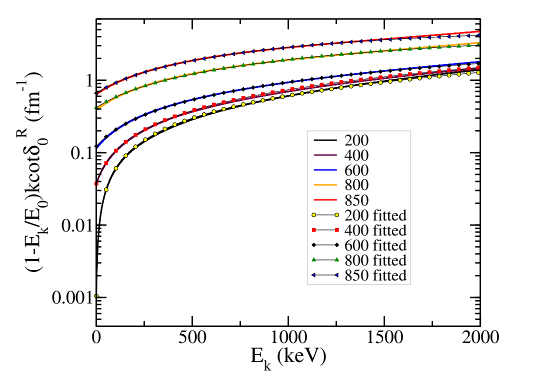

Pole positions in $k\cot\delta_0$ as a function of E_{nc}

From Braaten and Hammer [Phys. Rep.428 (2006) 259] for atom-dimer, we have

$$a_{AD} = (1.46 - 2.15\tan[s_0 \ln(a\Lambda_*) + 0.09])a.$$

$$a_0/a_B = \exp\left(\frac{\pi/2 - 0.59654}{s_0}\right)$$

a_B where one Efimov state is at the threshold, and a_0 where the atom-dimer scattering length is zero, or the pole in $k\cot\delta_0$ is at zero scattering energy, can be extended to the case of the $n - n - {}^{18}C$ system, when $a_{nn}^{-1} = 0$. For this mass imbalanced case $s_0 = 1.12$ with $A = 18$, and the analogous of the ratio a_B/a_0 is $\sqrt{E^0_{19C}/E^B_{19C}}$,

$$\sqrt{E^B_{19C}/E^0_{19C}} \approx \exp\left(-\frac{\pi/2 - 0.59654}{1.12}\right) = 0.419\,.$$

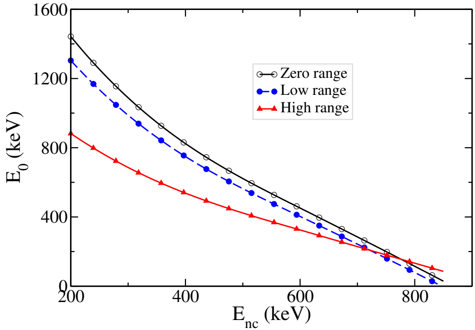

For the low-range potential, $E^0_{19C} = 850$ keV and $E^B_{19C} = 167$ keV r esulting $\sqrt{E^B_{19C}/E^0_{19C}} = 0.44$ and for high-range potential $E^0_{19C} = 940$ keV and $E^B_{19C} = 190$ keV resulting $\sqrt{E^B_{19C}/E^0_{19C}} = 0.45$,

Effective-range expression

$$k \cot \delta_0^R = \frac{-a^{-1} + b\, E_K + c\, E_K^2}{1 - E_K/E_0} = \frac{d}{1 - \frac{E_K}{E_0}} + e + f\, \frac{E_K}{E_0},$$

- residue: $d = -\frac{1}{a} + bE_0 + cE_0^2$
- $e = -bE_0 - cE_0^2$
- $f = -cE_0^2$

Parameters for the effective-range fitting – zero-range results.

Table: Effective-range parameters, obtained by fitting the effective-range expression to the results shown for the case that we have zero-range interactions, for a few values of $|E_{^{19}\mathrm{C}}|$ (first column).
Adjusting the table given in Yamashita et al. PLB 670, 49 (2008).

$\lvert E_{^{19}\mathrm{C}}\rvert$ (keV)	$-1/a$ (fm^{-1})	b (fm.keV)$^{-1}$	c (fm.keV^2)$^{-1}$	E_0 (keV)
200	$5.155 \cdot 10^{-3}$	$5.498 \cdot 10^{-4}$	$5.995 \cdot 10^{-8}$	1442.6
400	$6.280 \cdot 10^{-2}$	$6.593 \cdot 10^{-4}$	$1.004 \cdot 10^{-7}$	823.89
600	0.220	$9.284 \cdot 10^{-4}$	$1.508 \cdot 10^{-7}$	451.40
800	1.299	$3.242 \cdot 10^{-3}$	$3.447 \cdot 10^{-7}$	114.981
850	5.624	$1.260 \cdot 10^{-2}$	$1.1921 \cdot 10^{-6}$	28.851

Parameters for the effective-range fitting − low-range, r_{nc}.

Table: Effective-range parameters, obtained by fitting Eq. (12) to Fig. 2, when considering different values of $|E_{^{19}\mathrm{C}}|$ (first column) with short-range Yamaguchi potentials.

$\lvert E_{^{19}\mathrm{C}}\rvert$ (keV)	$-1/a$ (fm^{-1})	b (fm.keV)$^{-1}$	c (fm.keV^2)$^{-1}$	E_0 (keV)	d (fm^{-1})	r_{nc} (fm)
200	$6.028 \cdot 10^{-3}$	$5.579 \cdot 10^{-4}$	$5.717 \cdot 10^{-8}$	1304	0.831	0.157
400	$6.555 \cdot 10^{-2}$	$6.742 \cdot 10^{-4}$	$9.144 \cdot 10^{-8}$	749.0	0.622	0.174
600	0.234	$9.840 \cdot 10^{-4}$	$1.316 \cdot 10^{-7}$	402.9	0.652	0.190
800	1.798	$4.467 \cdot 10^{-3}$	$3.519 \cdot 10^{-7}$	78.86	2.153	0.205
830	5.149	$1.198 \cdot 10^{-2}$	$8.578 \cdot 10^{-7}$	28.98	5.497	0.208

Parameters for the effective-range fitting − high-range, r_{nc}.

Table: Effective-range parameters, obtained by fitting Eq. (12) to Fig. 2, when considering different values of $|E_{^{19}\mathrm{C}}|$ (first column) with high-range Yamaguchi potentials.

$\lvert E_{^{19}\mathrm{C}}\rvert$ (keV)	$-1/a$ (fm^{-1})	b (fm.keV)$^{-1}$	c (fm.keV^2)$^{-1}$	E_0 (keV)	d (fm^{-1})	r_{nc} (fm)
200	$5.020 \cdot 10^{-3}$	$5.267 \cdot 10^{-4}$	$7.580 \cdot 10^{-8}$	881.9	0.528	2.736
400	$4.216 \cdot 10^{-2}$	$6.319 \cdot 10^{-4}$	$2.806 \cdot 10^{-8}$	537.7	0.390	3.233
600	0.122	$8.395 \cdot 10^{-4}$	$-2.372 \cdot 10^{-8}$	324.8	0.392	3.720
800	0.405	$1.746 \cdot 10^{-3}$	$-2.332 \cdot 10^{-7}$	132.9	0.633	4.255
850	0.661	$2.603 \cdot 10^{-3}$	$-4.228 \cdot 10^{-7}$	85.60	0.880	4.403

The $s-$wave absorption parameter $\eta = |e^{2i\delta_0}|$ as a function of projectile neutron energy

- left frame: zero–range potential
- middle frame: low–range Yamaguchi potential (with large β)
- right frame: high–range Yamaguchi potential (with small β)

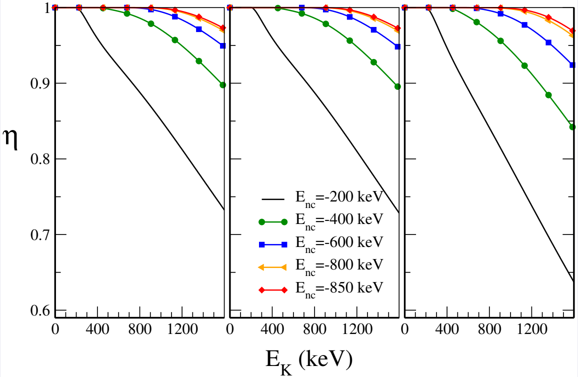

The $s-$wave elastic $n - nc$ cross section as a function of projectile neutron energy

- red solid lines: Yamaguchi potential with low β
- blue dashed-lines: Yamaguchi potential with high β
- black dash-dotted lines: zero-range

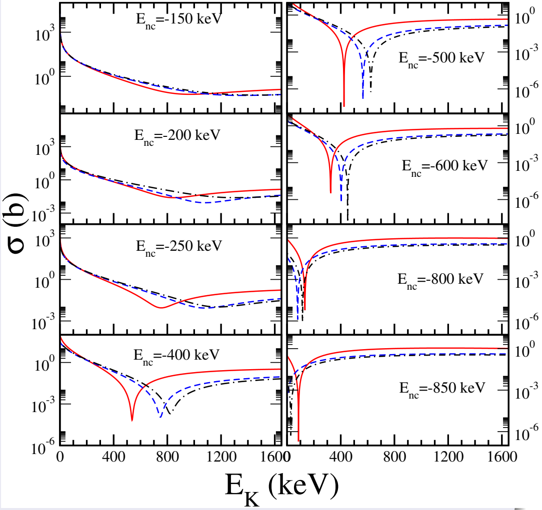

Resume for the case of $n-{}^{20}$C scattering

- We investigated the low-energy properties of the elastic $s-$wave scattering for the neutron$-{}^{19}$C near the critical condition for the occurrence of an excited Efimov state.
- Our calculations extends a zero-range approach to finite-range two-body interactions, where it was shown that the real part of the elastic $s-$wave phase shift (δ_0^R) reveals a zero when the $n-n-c$ system is close to an excited Efimov state (bound or virtual).
- We verified that by considering a finite-range potential, the results for the $s-$wave scattering amplitude present universal scaling features, with the variation of the ^{19}C binding energy for fixed ^{20}C and neutron-neutron singlet virtual state energies.
- The scaling of the effective-range parameters and the pole position of $k\cot\delta_0^R$, are in general consistent with the scaling of the zero-range potential, but the variation of this parameters shows less sensitivity to the variation of $n-{}^{18}C$ subsystem energy for higher range values.
- The ratio $\sqrt{E^B_{^{19}C}/E^0_{^{19}C}}$ obtained for finite range potentials changing from 0.44 to 0.45 are close to the universal ratio ≈ 0.419.

- The excited three-body ^{20}C state turns into a virtual state for a large ^{19}C binding, the threshold moves from 167 keV to 190 keV when the effective ranges are increased to reasonable physical values.
- We have also clarified that the analytical structure of the unitary cut is not affected by the potential range or mass asymmetry of the three-body system.
- We move to atoms this approach with mass-imbalanced three-particle systems, in view of the actual interest in verifying Efimov physics with different mixing of atomic species.

Efimov Physics in weakly-bound atomic systems

- Investigations of Efimov physics in atomic systems have being studied by several groups. One of the focus have been the ^{4}He trimer, which was suggested having an excited Efimov state by Cornelius and Gloeckle [J. Chem.Phys. 85, 3906 (1986)].
- Observation of such Efimov state was recently reported by Kunitski et al., Science 348, 551 (2015).
- The studies of Helium trimer have a long story, with realistic calculations been performed by Kolganova, Motovilov and Sofianos [Phys.Rev.A 56, R1686 (1997)]. See also, Kolganova, Phys. of Part. Nucl., 1108 (2015); and Kolganova, E. A.; Motovilov, A. K.; Sandhas, Few-Body Syst. 51, 249 (1989).

Atomic weakly bound three-body systems

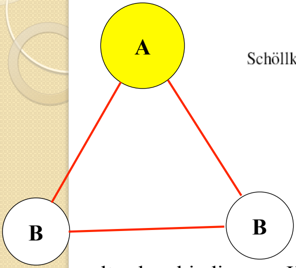

Schöllkopf, W., Toennies, J. P.: Science **266**, 1345 (1994)

dimer $R_{^4He-^4He} \sim 50$ A

A-B-B weakly bound molecules

ultra-low binding ~ mK or < mK

$^{133}Cs_3$ (trapped ultracold gas near a Feshbach resonance)

$^4He_3$ $^4He_2 - {}^7Li$ $^4He_2 - {}^6Li$ $^4He_2 - {}^{23}Na$

Delfino, Frederico and L.T., "Prediction of a weakly bound excited state in the $^4He_2$-^7Li Molecule", J. of Chem. Phys. 113 (2000) 7874.

26

Motivations from ultracold atom laboratories

- In the unitary limit, two levels are related by an exponential scaling factor $\exp(2\pi/s_0)$, where s_0 is a constant that varies according to the mass-ratio m_H/m_L. For $m_H = m_L$, the energy-ratio is predicted to be ~ 515, such that it will be quite difficult for an experimental verification.
- Optimal situations can occur for $m_H \gg m_L$.
- In case of $m_H = 100 m_L$, the ratio between consecutive levels of the bound-state energy spectrum is given by $\exp(2\pi/s_0) \sim 4.7$.
- We show that the discrete Efimov scaling factor can be well identified in the corresponding scattering observables of one atomic species α when colliding with a two-body $\alpha\beta$ bound-state.
- Our present results can be quite relevant for the going-on experimental observations of Efimov physics in cold-atom laboratories.

Motivations from ultracold atom laboratories

- Heidelberg group is studying the extreme mass-imbalance mixtures composed by ^{133}Cs and ^{6}Li atomic species [J. Ulmanis et al, PRL **117** (2016) 153201].
- Ultracold degenerate mixtures of alkali-metal-rare-earth molecules, ^{174,173}Yb$-^{6}$Li have also been considered by H. Hara et al [PRL **106** (2011) 205304] and Hansen et al [PRA **84** (2011) 011606(R)].
- Therefore, we understand that more favorable conditions are accessible to probe the rich Efimov physics in cold-atom laboratories. with low-energy collision of a heavy atom in a weakly-bound molecule as LiCs or LiYb.
- Note that, for the above mentioned examples, we have mass-ratios as m_L/m_H =0.034 for LiYb and 0.045 for LiCs

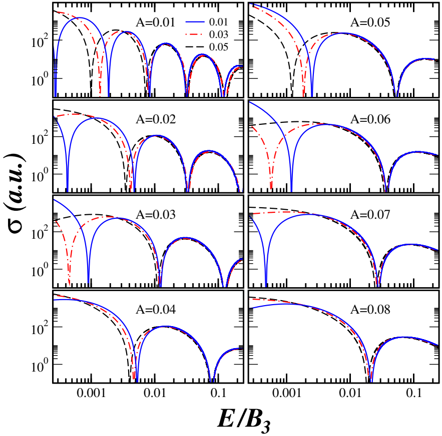

Figure: Results obtained for σ (in arbitrary units) as a function of the collision energy (in units of $\mathcal{B}_3$), for three values of the $\alpha\beta$ binding energy, $B_{\alpha\beta}/\mathcal{B}_3$ =0.01 (solid-blue lines), 0.03 (dot-dashed-red lines) and 0.05 (dashed-black lines), given in eight panels. Each panel is for a given fixed value of the mass-ratio $A \equiv m_\beta/m_\alpha$ (indicated inside the panels).

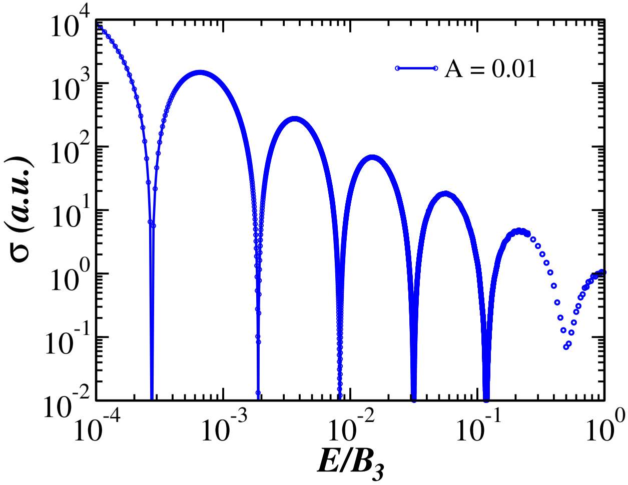

Figure: The case that $m_\beta/m_\alpha = 0.01$, with $B_{\alpha\beta}/\mathcal{B}_3 = 0.01$.

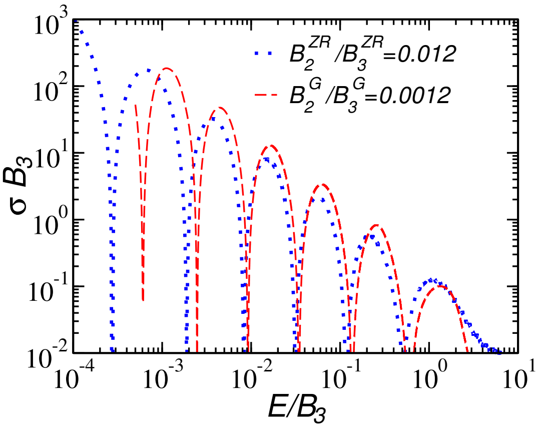

Figure: s-wave cross-section as a function of E/B_3, corresponding to $m_L/m_H = 0.01$, $B_{HL}/\mathcal{B}_3 = 0.01$ (zero-range) and $B_{HL}/\mathcal{B}_3 = 0.0012$ (Gaussian). The values of σ are obtained with zero-range (solid-blue lines) and Gaussian (dashed-red lines) potentials.

Table: Energy positions, $E^{(n)}/\mathcal{B}_3$, for the zeros of σ, for $B_{HL}/\mathcal{B}_3 =$0.01. In the last column we have energy ratios, with corresponding unitary limit in parenthesis.

A	$n=5$	$n=4$	$n=3$	$n=2$	$n=1$	$\frac{E^{(n+1)}}{E^{(n)}}$(ul)
0.01	0.117488	0.031569	0.008279	0.001886	0.000275	$\rightarrow$3.7(4.7)
0.02	-	0.220402	0.032841	0.004805	0.000424	$\rightarrow$6.7(8.7)
0.03	-	-	0.125390	0.012351	0.000905	$\rightarrow$10.2(13.6)
0.04	-	-	-	0.079298	0.005296	$\rightarrow$15.0(19.5)
0.05	-	-	-	0.053320	0.002500	$\rightarrow$21.3(26.4)

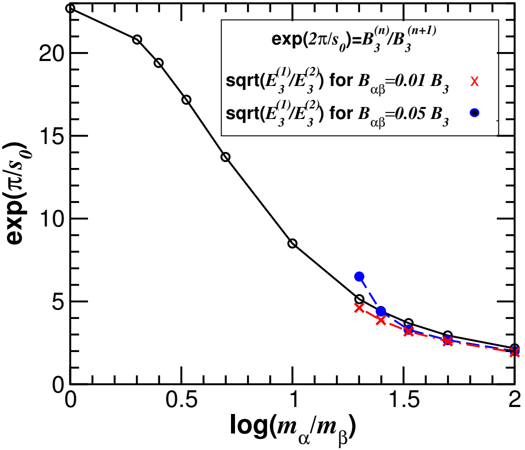

Figure: The ratios between the scattering energies corresponding to the positions of the zeros for the cross-section are shown with blue bullets, in the same plot already verified for the Efimov spectrum, when varying the mass ratio.

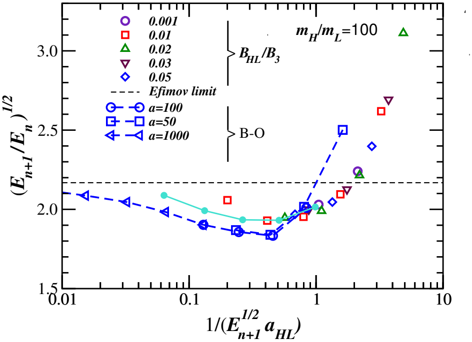

Figure: Adiabatic (blue-dashed curve) and zero-range Faddeev calculations (symbols shown inside) for $m_H/m_L = 100$. Scaling plot, with the ratios between consecutive energy-poles of $k \cot \delta_0$, where $k^2 = (m_H/\hbar^2)E_k$) and $1/(k_n a_{HL}) \approx \sqrt{\frac{2B_{HL}}{100E_n}}$.

Final remarks

- The poles of $k \cot \delta_0$ (zeros/minima of the $s-$wave cross section) are shown to be directly connected with the Efimov spectrum of the heavy-heavy-light system near the unitary limit.
  This is shown by considering a mass-imbalanced system $A << 1$ with no interaction between the two-heavy particles and with the heavy-light sub-system bound with energy close to zero.
- By considering the mass ratio between Li and Yb, $A =$0.034, the cross-section for the Yb + LiYb collision can in principle present a couple of zeros. We can imagine a situation where $a_{\mathrm{YB-Li}}$ is adjusted at some large positive values, with the colliding energy being varied slowly.
- The challenge in cold-atom experiments would be to control the scattering length towards the large values and then observe the cross-section minima at geometrically spaced colliding energies.

THANKS![1]

[1] Work supported by the Brazilian agencies CAPES, CNPq and FAPESP

Adiabatic approach for two heavy and one light particle

For the purpose to show how the inverse square interaction emerges in the low-energy three-body problem, we consider two identical heavy particles (1 and 2) with equal masses M, with the third particle (3) having mass $m \ll M$. From the corresponding coordinates, $\mathbf{r}_1$, $\mathbf{r}_2$, and $\mathbf{r}_3$, by introducing the relative ones $\mathbf{R} = (\mathbf{r}_1 - \mathbf{r}_2)$ and $\mathbf{r} = \left(\mathbf{r}_3 - \frac{\mathbf{r}_1+\mathbf{r}_2}{2}\right)$, as well as taking $M \gg m$ and units such that $\hbar = 2m = 1$, we can write the three-body Schrödinger equation as

$$H\Psi(\mathbf{r},\mathbf{R}) = \left[-\frac{\nabla_R^2}{\mu} - \frac{\nabla_r^2}{\nu} + \sum_1^3 V_i\right]\Psi(\mathbf{r},\mathbf{R}), \tag{1}$$

where $\mu \equiv M/(2m)$, $\nu \equiv 2M/(2M+m)$ and V_i are the interactions between particles j and k ($i \neq j \neq k = 1, 2, 3$). As the heavy particles are very slow in comparison with the light particle, we apply the Born-Oppenheimer approximation, by decomposing the wave function as $\Psi(\mathbf{r},\mathbf{R}) = \psi_{\mathbf{R}}(\mathbf{r})\phi(\mathbf{R})$, where $\mathbf{R}$ is a parameter in $\psi_{\mathbf{R}}(\mathbf{r})$. In this way, the solution of the equation for the light-heavy particle system will provide the adiabatic potential, $\mathcal{E}(R)$, for the two heavy particles. The coupled system is given by

$$\begin{aligned}
&\left[-\frac{\nabla_r^2}{\nu} + \sum_{i=1,2} V_i\left(\left|\mathbf{r} + (-1)^i\frac{\mathbf{R}}{2}\right|\right) - \mathcal{E}(R)\right]\psi_{\mathbf{R}}(\mathbf{r}) = 0\\
&\left[-\frac{\nabla_R^2}{\mu} + V_3(R) + \mathcal{E}(R)\right]\phi(\mathbf{R}) = E_3\,\phi(\mathbf{R}).
\end{aligned} \tag{2}$$

The asymptotic behavior of $\mathcal{E}(R)$ is not affected by $V_3(\mathbf{R})$, such that one can assume $V_3(\mathbf{R}) = 0$. For the light-heavy particles one can take short-range separable interactions, with V_1 and V_2 having the operator form $\lambda|g\rangle\langle g|$. The light-heavy particle system, which can easily be solved in momentum space by considering Yamaguchi form-factors with $g(p) \equiv (p^2+\beta^2)$, it is assumed a shallow bound state with $B_{\alpha\beta} = \hbar^2/(2ma_{\alpha\beta}^2)$, where $a_{\alpha\beta} \equiv a$ is the light-heavy scattering length. The scattering length for the two-body sub-system is assumed to be infinite.

Adiabatic approach for two heavy and one light particle

The effective potential $\mathcal{E}(R)$ (considering $V_3(R) = 0$) in the equation for $\phi(\mathbf{R})$, within the Born-Oppenheimer approximation [5] and scaling limit, is given by

$$\mathcal{E}(R) = -\frac{\hbar^2}{2m\nu}\kappa^2, \quad \text{where} \quad \kappa \equiv \kappa(R) \quad \text{and} \quad \left[\kappa - \frac{1}{a}\right] R = e^{-\kappa R}. \tag{3}$$

The solution in the limit $a \to \infty$ leads to

$$\mathcal{E}(R) = -\frac{\hbar^2}{2m}\frac{A^2}{\nu R^2}, \quad \text{where} \quad A = e^{-A} = 0.5671433. \tag{4}$$

The expression for $\kappa(R)$, can also be fitted by considering arbitrary values of a, which will give us

$$\kappa(R) \approx \frac{1}{a} + \left(\frac{A}{R} + \frac{c}{a}\right) e^{-\frac{R}{a}}, \tag{5}$$

where $c \equiv 0.185$. With this, the effective expression,

$$\mathcal{E}(R) = -\frac{\hbar^2}{2m\nu a^2}\left[1 + \left(\frac{Aa}{R} + c\right) e^{-\frac{R}{a}}\right]^2, \tag{6}$$

will satisfy both limits $R << a$ and $R >> a$. In the limit $R << a$, the radial equation for the two heavy is

$$\frac{\hbar^2}{M}\left[-\frac{d^2}{dR^2} - \left(\frac{2M+m}{4m}\right)\frac{A^2}{R^2}\right] u = E_3 u, \tag{7}$$

where $u \equiv u(R) \equiv R\phi(\mathbf{R})$.

Adiabatic approach for two heavy and one light particle

For a radial potential Λ/R^2, where Λ is dimensionless, the system has no bound-state for $\Lambda > -1/4$, and is anomalous for $\Lambda < -1/4$ due to the singularity at $R \to 0$. There is no lower limit in the energy spectrum, which requires a regularization, such that $R > r_c$, where r_c is a radial cut-off. Therefore, for a boundary condition we fix the wave function to zero at $R = r_c$. Important to note that the geometric scaling property is independent on the value of r_c. So, we will rewrite Eq. (7) as

$$\left[-\frac{d^2}{dR^2} - \frac{s_a^2 + \frac{1}{4}}{R^2}\right] u = \frac{M}{\hbar^2} E_3 u = k^2 u, \quad \text{where} \tag{8}$$

$$s_a = \sqrt{\frac{2M + m}{4m} A^2 - \frac{1}{4}}, \quad \text{and} \quad k \equiv \sqrt{\frac{ME_3}{\hbar^2}}. \tag{9}$$

Here, we use the definition s_a corresponding to the exact numerical factor, usually defined as s_0. Let us check the numerical values obtained from (9), for a few values of $M \gg m$, in comparison with the values of s_0 given in Braaten and Hammer, Phys. Rep. 428 (2006) 259:

Table: Values of the scaling factor s_a and $e^{\frac{\pi}{s_a}}$, obtained by the adiabatic expression (9) in comparison with the respective exact values. Note that, the scaling for the energies are $e^{\frac{2\pi}{s_a}} = 4.83$ ($s_a = 3.99$) in the adiabatic case, with $e^{\frac{2\pi}{s_0}} = 4.70$ ($s_0 = 4.06$) for the exact case.

m/M	0.1	0.05	0.04	0.03	0.02	0.01	0.001
s_a	1.1995	1.7456	1.9624	2.2784	2.8057	3.9891	12.675
s_0	1.4682	1.9194	2.1142	2.4067	2.9084	4.0612	12.698
$e^{\frac{\pi}{s_a}}$	13.725	6.0483	4.9574	3.9703	3.0641	2.1980	1.2813
$e^{\frac{\pi}{s_0}}$	8.4977	5.1383	4.4193	3.6889	2.9452	2.1675	1.2807

Adiabatic approach for two heavy and one light particle

For the case of bound-states with $E_3 = -\mathcal{B}_3 = -\frac{\hbar^2}{M}\kappa^2$, the solutions are given by the zeros of a modified Bessel function of the third kind with pure imaginary order $\mathrm{i}s_0$, $u(R) = \sqrt{\kappa R}K_{\mathrm{i}s_0}(\kappa R)$. As the wave function must be zero at the boundary condition, where $R = r_c$, this is satisfied by discrete values of $\kappa = \kappa_n$, where $K_{\mathrm{i}s_0}(\kappa_n r_c) = 0$, emerging the geometric scaling of the spectrum:

$$\frac{\mathcal{B}_3^{(n)}}{\mathcal{B}_3^{(n+1)}} = e^{2\pi/s_0} \quad (n = 0, 1, 2, \ldots). \tag{10}$$

In the scattering case, when $E_3 = \frac{\hbar^2}{M}k^2$, the solution for Eq. (8) can be found in the on-line *WolframAlpha General Differential Equation Solver* in terms of Bessel functions $J_\nu(z)$:

$$u(R) = \sqrt{R}\left[c_1 J_{\mathrm{i}s_0}(kR) + c_2 J_{-\mathrm{i}s_0}(kR)\right], \tag{11}$$

where c_1 and c_2 are arbitrary constants, which can be given by the normalization of the wave function and continuity of the logarithmic derivative. First, the ratio c_2/c_1 can be given by the condition that $u(R)$ is zero for some fixed $R = 1$. Next, we fix the conditions for the continuity of the logarithmic derivative at $R = a \gg 1$. With $z \equiv ka$, we have the following expressions to obtain the $s-$wave phase shifts $\delta_0 \equiv \delta_0(k)$:

$$z\cot(z+\delta_0) = \frac{1}{2} + z\left[\frac{J'_{\mathrm{i}s_0}(z)J_{-\mathrm{i}s_0}(k) - J_{\mathrm{i}s_0}(k)J'_{\mathrm{i}s_0}(z)}{J_{\mathrm{i}s_0}(z)J_{-\mathrm{i}s_0}(k) - J_{\mathrm{i}s_0}(k)J_{-\mathrm{i}s_0}(z)}\right]_{z=ka}$$

Adiabatic approach for two heavy and one light particle

Here we should note that the continuity of the logarithmic derivative of the wave-function was done at $R = a$, such that an error is expected in the results, because we have used $R \ll a$ in the expansion for Eq. (6). In order to improve this approximation, our effective potential will include a Coulomb-like $1/R$ interaction, with the Eq. (8) being replaced by

$$\left(-\frac{d^2}{dR^2} - \frac{s_0^2 + \frac{1}{4}}{R^2}\left[g\left(\frac{R}{a}\right)\right]\right) u = \frac{M}{\hbar^2} E_3 u = k^2 u, \quad \text{with}$$
$$\text{where} \quad g(y) \approx 1 + c_1 y + c_2 y^2. \tag{12}$$

As our approximation should be valid not only for $R \ll a$, but also for $R/a \sim 1$, we need to adjust the potential (6) by a fitting. In case of a fitting valid up to $R \sim 3a$, we have $g(y) \approx 1 + 1.64y + 2.43y^2$. However, the third term of $g(y)$ is relevant for the fitting of the effective potential for large values of a, such that can be ignored as it is independent on R and proportional to $1/a^2$. Therefore, it is better to improve the approximation for smaller values of R, with almost exact values for R/a =0, 0.5 and 1. This can be done with

$$g(y) \approx 1 + 2y + 2.07y^2. \tag{13}$$

The correction we need to add to the potential $1/R^2$ is $-2\left(s_0^2 + 1/4\right)/(aR)$. With this term in Eq. (12), the solutions are given by Whittaker functions, such that

$$u(R) = c_1 M_{-\mathrm{i}B,-\mathrm{i}s_0}(2\mathrm{i}kR) + c_2 W_{-\mathrm{i}B,-\mathrm{i}s_0}(2\mathrm{i}kR),$$

where $B \equiv (s_0^2 + \frac{1}{4})\frac{1}{ka}$. The Whittaker functions M and W can be written in terms of a confluent hypergeometric functions ${}_1F_1(a_1, a_2; z) \equiv M(a_1, a_2, z)$ and $U(a_1, a_2, z)$:

$$(M, W)_{-\mathrm{i}B,\mathrm{i}s_0}(2\mathrm{i}kR) = e^{-\mathrm{i}kR}(2\mathrm{i}kR)^{\frac{1}{2}+\mathrm{i}s_0}(M, U)\left(\frac{1}{2} + \mathrm{i}s_0 + \mathrm{i}B, 1 + 2\mathrm{i}s_0, 2\mathrm{i}kR\right).$$

Adiabatic approach for two heavy and one light particle

Therefore,

$$u(R) = e^{-\mathrm{i}kR}(2\mathrm{i}kR)^{\frac{1}{2}-\mathrm{i}s_0} \times \left\{c_1 M\left(\frac{1}{2}-\mathrm{i}s_0+\mathrm{i}B, 1-2\mathrm{i}s_0, 2\mathrm{i}kR\right)+c_2 U\left(\frac{1}{2}-\mathrm{i}s_0+\mathrm{i}B, 1-2\mathrm{i}s_0, 2\mathrm{i}kR\right)\right\}. \quad (14)$$

To write the two components of $u(R)$ in terms of the same function M, we can use the relation

$$U(a_1, a_2, z) = \frac{\Gamma(1-a_2)}{\Gamma(1+a_1-a_2)} M(a_1, a_2, z) + \frac{\Gamma(a_2-1)}{\Gamma(a_1)} z^{(1-a_2)} M(a_1-a_2+1, 2-a_2, z).$$

For the derivative of $u(R)$, we can use the relation

$$\frac{d}{dz} M(a_1, a_2, z) = \frac{a_1}{a_2} M(a_1+1, a_2+1, z).$$

$$\left.\frac{1}{u}\frac{du}{dR}\right|_{R=a} = -\mathrm{i}k + \frac{\frac{1}{2}-\mathrm{i}s_0}{a} + \left(\mathrm{i}k - \frac{\frac{1}{2}+\mathrm{i}s_0}{a}\right)\left\{\frac{U_0 M_+ + (1-\mathrm{i}s_0)M_0 U_+}{U_0 M - M_0 U}\right\}_{R=a}, \quad (15)$$

where $M \equiv M(a_1, a_2, 2\mathrm{i}kR)$, $U \equiv U(a_1, a_2, 2\mathrm{i}kR)$, $M_+ \equiv M(a_1+1, a_2+1, 2\mathrm{i}kR)$, $U_+ \equiv U(a_1+1, a_2+1, 2\mathrm{i}kR)$, $M_0 \equiv M(a_1, a_2, 2\mathrm{i}k)$, $U_0 \equiv U(a_1, a_2, 2\mathrm{i}k)$, with $a_1 \equiv \left(\frac{1}{2}-\mathrm{i}s_0\right)\left(1-\frac{\frac{1}{2}+\mathrm{i}s_0}{\mathrm{i}ka}\right)$ and $a_2 \equiv 1-2\mathrm{i}s_0$.

Adiabatic approach for two heavy and one light particle

The continuity of the logarithmic derivative implies

$$
\begin{aligned}
\delta_0 &= -ka + \cot^{-1}\left(\frac{1}{ku}\frac{du}{dR}\bigg|_{R=a}\right) = -ka + \theta \\
\cot\delta_0 &= \frac{\cot(ka)\cot\theta + 1}{\cot(ka) - \cot\theta} \\
\cot\theta &= \left(\frac{1}{ku}\frac{du}{dR}\bigg|_{R=a}\right) \qquad (16)
\end{aligned}
$$

Therefore, the zeros os $1/(k\cot\delta_0)$ are given by

$$
\cot(ka) = \left(\frac{1}{ku}\frac{du}{dR}\bigg|_{R=a}\right). \qquad (17)
$$